The Journal of Engineering

The 7th International Conference on Renewable Power Generation (RPG 2018)

IET Journals
The Institution of Engineering and Technology

Thermal modelling of a small wind turbine gearbox for condition monitoring

eISSN 2051-3305
Received on 26th October 2018
Accepted on 10th January 2019
E-First on 27th June 2019
doi: 10.1049/joe.2018.9282
www.ietdl.org

Becky Corley[1] ✉, *James Carroll*[1], *Alasdair McDonald*[1]

[1]*Wind Energy and Control Centre, University of Strathclyde, Glasgow, UK*

✉ *E-mail: Becky.Corley@strath.ac.uk*

Abstract: This study details the development of a mathematical thermal model of a small wind turbine gearbox for use in condition monitoring. The model was optimised and partially validated using experimental data from a wind turbine drivetrain test rig. The model was then used to mimic bearing faults, by simulating additional heat losses at respective faulty components. The extent to which the thermal behaviour changed as a result of a fault was studied, with a view to use such an approach to detect and locate faults.

Nomenclature

P_a	power (W)
n	rotational speed (rpm)
c	specific heat capacity (J kg^{-1} K^{-1})
T	temperature (K)
m	mass (kg)
b	tooth width (mm)
b_0	reference width (10 mm)
Q	heat flow (W)
v_t	peripheral speed at pitch circle (m/s)
v_{t0}	reference speed (10 m/s)
d_m	mean bearing diameter (mm)
d_{sh}	shaft diameter (m)
v_{oil}	kinematic viscosity of oil (mm^2/s)
F_a	bearing thrust load (N)

1 Introduction

In this work, the authors propose creating a mathematical model of a wind turbine gearbox so that when a fault occurs, the failure can be diagnosed, located and a prognosis can be developed. Through this modelling, a better understanding of the physics of failure will be obtained allowing failure prediction and in turn, reduce downtime when a failure occurs. This is especially useful when historical operational data is unavailable and/or diagnostic/prognostic models are transferred from other gearbox types. Thermal modelling based on the principles of heat transfer theory is used to develop this understanding, exploiting temperature measurements to understand a 'healthy' gearbox and then use it to detect and locate abnormal gearbox operating conditions.

2 Background

Wind turbine gearboxes operate under conditions subject to a broad spectrum of load and speed variations creating difficulties in predicting reliability and preventing failures [1]. Gearbox failure incurs high costs for repair in addition to lost revenue from high downtime per failure. The lengthy lead time and time typically cause an increase in the cost of energy [2].

Condition monitoring refers to processes that focus on early detection of faults, failures and wear of machinery with the intention of minimising downtime, operation and maintenance costs while maximising production [3]. Different techniques have been applied to diagnose gearbox failures in the main looking at vibration, oil quality and temperature with thresholds on sensor outputs used as fault indicators. State of the art remaining useful life methodologies predominately use data-driven machine learning techniques to predict failure, these so-called 'black box' approaches rely on large amounts of operational data and failure histories. The variable speed nature of modern wind turbine operation can be challenging for a conventional spectral-based method of fault diagnosis [4].

Exploiting temperature measurements to detect abnormal gearbox operating conditions is based on the theory that gearboxes generate power losses in the form of heat. It can be assumed that any degradation on the contact surface will generate more losses and thus a different thermal distribution will occur [5]. Most modern wind turbines (which use gearboxes) measure the gearbox temperature as a proxy of gearbox health.

Table 1 Gearbox specifications

rated power	17. 7 kW
gearbox ratio	18
type	2 stage, parallel axis
lubrication	oil splash
orientation	vertical

3 Method

The gearbox used in the study is from an 11 kW wind turbine. Relevant technical details of the gearbox are listed in Table 1.

3.1 Thermal modelling

The gearbox is modelled in MATLAB Simulink using the Simscape package. Thermal network modelling can be equated to electrical circuit theory by analogy where resistance to heat transfer is equivalent to electrical resistance, heat flow equates to current, temperature difference is equivalent to the potential difference and thermal mass to capacitance [6].

To create the thermal model, the gearbox components are split into a number of lumped mass isothermal nodes. The heat transfer between nodes is shown in Fig. 1, where the black lines represent the component nodes, labelled at the top of the figure. Linking these nodes are thermal resistances, representing heat transfer by conduction, convection and radiation. Losses are introduced at the respective nodes. Heat flows between nodes can be calculated, as temperature differences.

3.1.1 Heat transfer: The heat propagation through the gearbox is made up of different modes of heat transfer which are used in the

thermal model as thermal resistances R_{th}, as shown by (1). The heat flow is via conduction, convention or radiation:

$$R_{th} = \frac{\Delta T}{Q} \tag{1}$$

Each component in the gearbox acts as a thermal mass, retaining heat. The change in flow is dictated by (2):

$$Q = \mathrm{cm}\frac{\mathrm{d}T}{\mathrm{d}t} \tag{2}$$

3.1.2 Power losses in a 'healthy' gearbox: To measure the heat propagation of the gearbox, heat needs to be inputted into the model. The model assumes that any power loss in the gearbox eventually appears in the form of heat. The losses are generated by rotating parts; the interaction between the shaft, gears and bearings and their interaction with the air and lubrication. The total losses from different component parts are a mixture of load dependent and load independent losses as shown in (3). Each loss type can be estimated numerically, for the difference gearbox stages:

$$\sum P_T = \sum P_{GD} + \sum P_{GI} + \sum P_{BD} + \sum P_{BI} + \sum P_S \tag{3}$$

P_{GD} is the load dependent gear losses, P_{GI} is the load independent gear losses, P_{BD} is the load dependent bearing losses, P_{BI} is the load independent bearing losses and P_S is the seal losses.

Load dependent gear losses: Gear contact losses occur when gear teeth are in contact. The standard ISO/TR 14179-2:2001 [7] for calculating thermal losses uses (4). It uses a gear loss factor (H_v) which accounts for gear geometry and a mean coefficient of friction (μ). This method is widely used in other literature relating to gearbox efficiency [6, 8, 9–11]:

$$P_{GD} = P_a \mu H_v \tag{4}$$

Load independent gear losses: Load independent gear losses are made up of air windage and oil churning. For splash lubricated gears, oil churning is considered a major source of power loss [12]. Churning is dependent on rotational speed, immersion depth in the sump and lubricant viscosity [8]. A simple approach to calculating churning losses in [7] is used, with equations (5)–(9):

$$P_{GI} = \sum_{i=1}^{\text{stage}} T_{Hi}\frac{\pi n_i}{30} \tag{5}$$

$$T_H = C_{S_P} C_1 \mathrm{e}^{C_2(\nu_t/\nu_{to})} \tag{6}$$

$$C_{S_P} = \left(\frac{4h_{e,\max}}{3h_c}\right)^{1.5}\frac{2h_c}{1h} \tag{7}$$

$$C_1 = 0.063\left(\frac{h_{e1}+h_{e2}}{h_{eo}}\right) + 0.0128\left(\frac{b}{b_o}\right)^3 \tag{8}$$

$$C_2 = \frac{h_{e1}+h_{e2}}{80h_{eo}} + 0.2 \tag{9}$$

where h_{e1} h_{e2}, h_{e0}, $h_{e,max}$, h_c and l_h are all related to the geometry of the gearbox and oil sump. This approach was used based on the gearbox information available from design drawings; there are other more detailed approximations of churning losses [9, 10, 12, 13]that could be used for future thermal model development.

Load dependent and load independent bearing losses: An experimental approach to bearing losses is used by Fernandes *et al.* [14]. Experimental data is used to estimate coefficients of friction that contribute to the total frictional torque which is split into rolling, sliding, seals and drag losses. This approach includes a number of numerical factors, unknown for this gearbox so the approach, described in [7] was used, as listed in (10)–(14):

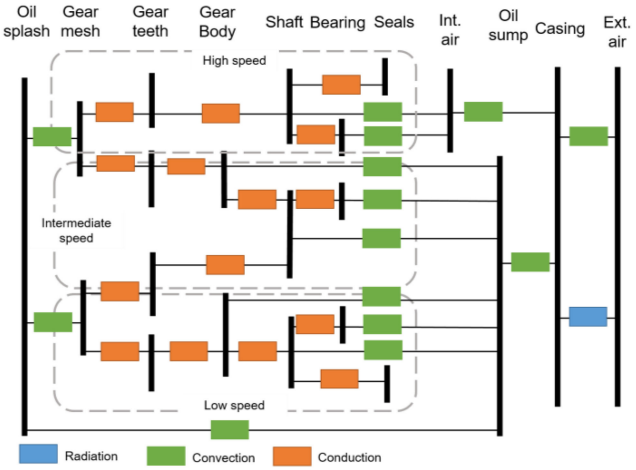

Fig. 1 *Thermal model network diagram*

$$T_B = T_{BL0} + T_{BLP1} + T_{BLP2} \tag{10}$$

Load independent:

$$\text{If } \nu_{oi1}\, n < 2000\frac{\mathrm{mm}^2}{\mathrm{s}}\frac{\mathrm{min}}{T_{BL0}} = 1.6\times 10^{-8} f_0 d_m^3 \tag{11}$$

$$\text{If } \nu_{oi1}\, n \geq 2000\frac{\mathrm{mm}^2}{\mathrm{s}}\frac{\mathrm{min}}{T_{BL0}} = 10^{-10} f_0 (\nu_{oil} n)^{2/3} d_m^3 \tag{12}$$

Load dependent:

$$T_{BLP1} = f_1 P_1^a d_m^b \times 10^{-3} \tag{13}$$

for radial loading

$$T_{BLP2} = 0$$

for cylindrical roller bearing additional thrust loading (F_a)

$$T_{BLP2} = f_2 F_a d_m \times 10^{-3} \tag{14}$$

where f_1, P_1, f_2 and a and B are from lookup tables in [7, 13].

Seal losses: Equation (15) is used widely for calculating contacting, radial shaft seals [7, 13]:

$$P_s = 7.69\times 10^{-6} d_{sh}^2 n \tag{15}$$

3.2 Experimental validation

Once the mathematical model was created, it was partially validated by experimental data using a wind turbine drive train test rig located at the University of Strathclyde. For operational wind turbine gearboxes, there are usually at least three temperature sensors installed: the main bearing, high-speed shaft bearing and gearbox oil [15]. As this gearbox is in the University lab, sensors can be added in more locations. Allowing for restrictions in the geometry of the gearbox, a sensor system was designed and installed to correspond to the individual gears and shafts. This configuration is shown in Fig. 2. These are held in very close proximity to the shafts and gears.

The test rig is made up of two identical gearboxes back to back, driven by a motor, controlled by a torque and speed control unit. One of the gearboxes is set up with the temperature sensors and a torque metre is fitted to the output shaft. The data acquisition instrumentation was made up of TMP35/6/7 temperature sensors connected to an Arduino Mega. The operating conditions were set at 968 N m and 57 rpm, giving an output power of 5.8 kW, approximately half the rated power of the small wind turbine it is designed for.

1.	High-Speed Shaft
2.	Intermediate Speed Gear
3.	Intermediate Speed Shaft
4.	Low-Speed Gear
5.	Low-Speed Shaft

Fig. 2 *Temperature sensor set-up*

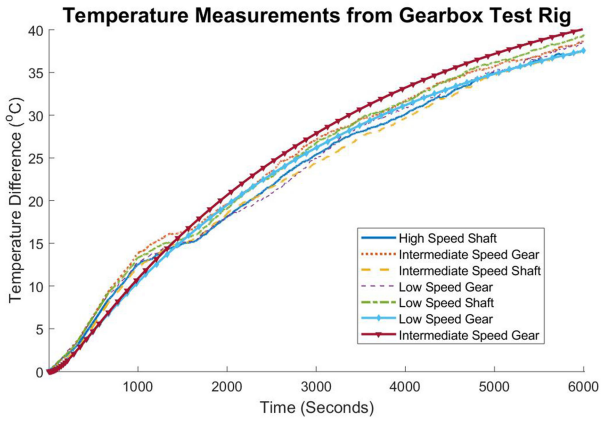

Fig. 3 *Experimental and numerical temperature measurements*

4 Results

4.1 Verification of model using a 'healthy' gearbox

To compare the experimental data with the thermal model, the data was filtered to remove the noise for a clearer comparison. Fig. 3 shows the temperature measurements as the difference from ambient temperature, from experimental data (solid lines) and thermal model (dashed lines). The temperature results from the thermal model at the gear nodes are in general agreement with the experimental model. In some cases, they were lower than those of the experimental data, suggesting either that the calculated losses at the gear meshes were underestimated in the model, that there are differences in the thermal resistance network or that the measurements are not accurate (e.g. due to indirect temperature measurement).

The experimental data shows all components increasing in temperature at a similar rate of change. There is a significant difference between the low speed and intermediate speed gears which is explained by the larger effective thermal resistance between the intermediate speed gears and ambient temperature as well as their different thermal capacities**.** It can be noticed that there is an inflection point in the experimental data between 1000 and 2000 s. It is postulated that this because as the temperature of the oil increases the viscosity reduces and the losses also drop. This feedback is not present in the model.

4.2 Further results from 'healthy' gearbox model

The thermal model can give temperature measurements for parts of the gearbox that would be difficult to access. Figs. 4 and 5 show the temperature of the gearbox bearings and the oil sump and casing, respectively. The model running time was increased from 6000 to 60,000 s to clearly see when thermal equilibrium is reached. It should be highlighted that due to the variable nature of wind turbine operation, a wind turbine gearbox would rarely be in thermal equilibrium.

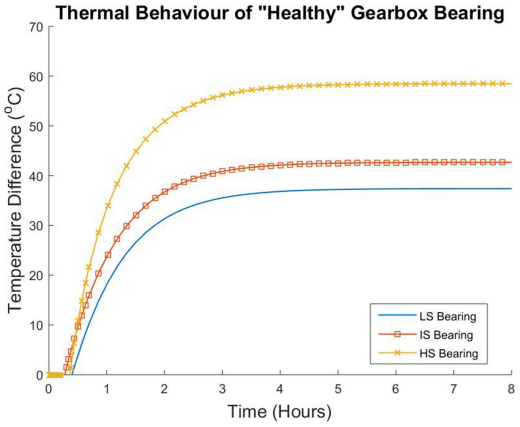

Fig. 4 *'Healthy' thermal model – bearings*

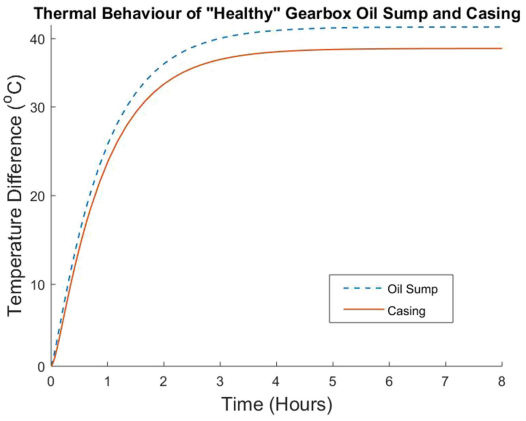

Fig. 5 *'Healthy' thermal model – oil sump and casing*

4.3 Use of thermal model to investigate gearbox 'fault'

The hypothesis that the model can be used to monitor a fault at the component level was tested. To do this, extra heat losses were introduced into the model at the high-speed (HS) bearing nodes to mimic fault heat. The bearing was selected in the first instance as is a common gearbox failure mode. Bearing failure cause around 70% of gearbox downtime [3]. The top failure modes for bearings from a case study [16] found the most common root causes are cracking, abrasion and adhesion/scuffing. To a certain degree, these faults will all affect the friction within the bearing and thus heat generated. However, the magnitude of this additional heat input in real gearboxes is unknown, it does not appear to be covered in available literature.

To model a fault in the high-speed bearing, an estimated approach has been taken, where a step increase in heat flow is added at the HS bearing node at 1/3 way into the total simulation when it has reached thermal equilibrium. The temperature increase of different levels of fault is shown in Fig. 6. An important outcome of the thermal model is to determine if a fault in a component can be detected elsewhere, for example, the oil sump. A location commonly used to monitor temperature for SCADA Fig. 7 shows oil sump temperature as a result of a 'fault' at the HS bearing temperature. These fault heat levels (10, 20 and 30 W) represent a 12.5, 25 and 37.5% increase in heat that is already present in the healthy gearbox.

The same 'Fault' process has been applied to the low-speed (LS) bearing in the model to compare Fig. 8. This gives a similar result but with a lower equilibrium temperature due to its slower rotational speed and lower equivalent thermal resistance. The thermal behaviour of the oil sump (Fig. 9) is almost identical to a fault in the high-speed bearing.

Figs. 8 and 9 show that using a single temperature measurement, such as the oil sump temperature does not give much information about a fault location. However, if the difference in temperature between the two components is used, it yields more useful information.

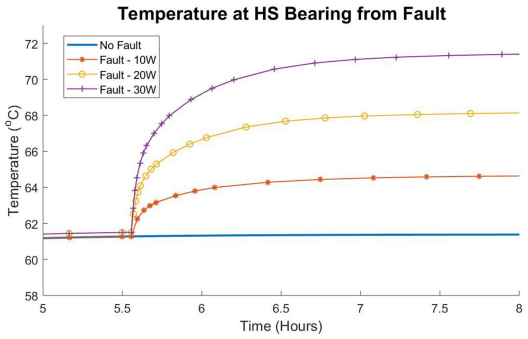

Fig. 6 *Effect of HS bearing 'Fault' on HS bearing temperature*

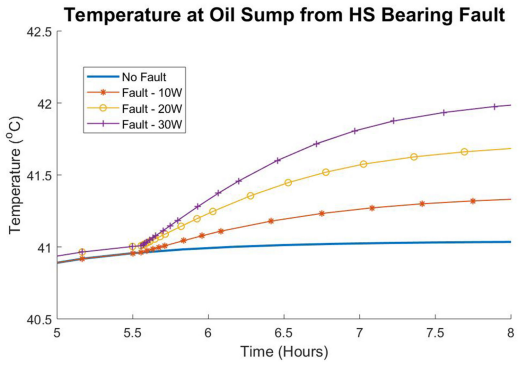

Fig. 7 *Effect of HS bearing 'Fault' on oil sump temperature*

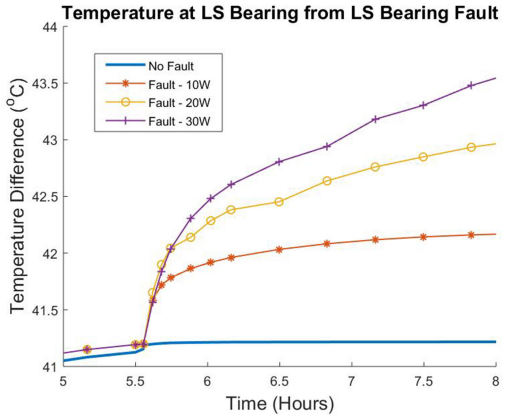

Fig. 8 *Effect of LS bearing 'Fault' on LS bearing temperature*

Figs. 10 and 11 show the difference in temperature between nodes, illustrating that faults in different locations produce different thermal behaviour. This suggests that multi-locational measurements alongside a thermal model should be able to locate faults.

It is suggested by de Azevedo *et al.* [3] that an effective way to reduce the effects of the load is to monitor the difference between temperatures of components since both temperatures would increase with load and, their difference should be less dependent on load variation. This idea can be used to develop the thermal model further, especially when considering a range of operating conditions.

5 Discussion

The preliminary nature of this stage of research means there are a number of simplifications and uncertainties.

5.1 Uncertainties

Thermal network models rely on simplifying the gearbox components but it can be argued that isothermal approaches that rely on oil sump temperature may underestimate gearbox efficiency because the contributions of local temperature rises are ignored.

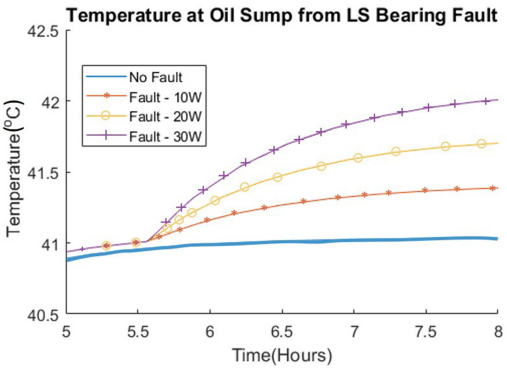

Fig. 9 *Effect of LS bearing 'Fault' on oil sump temperature*

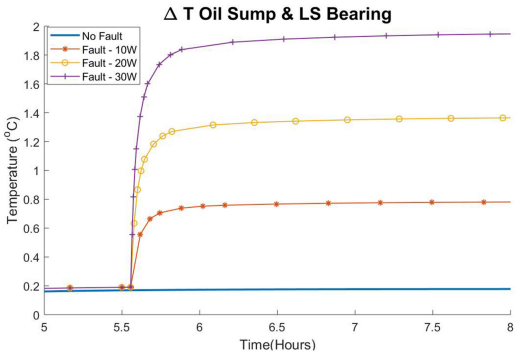

Fig. 10 *Temperature difference between LS bearing and oil sump due to fault at LS bearing*

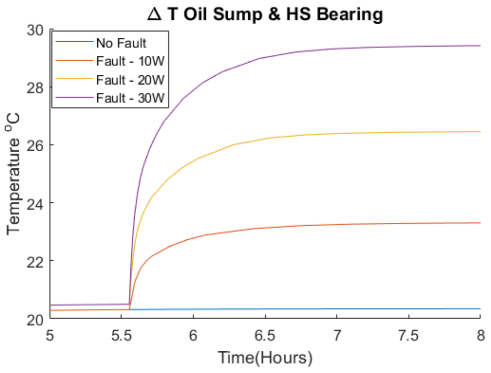

Fig. 11 *Temperature difference between HS bearing and oil sump due to fault at HS bearing*

Durand de Gevigney *et al.* [6] suggest dividing the gearbox into a number of isothermal parts to account for these variations.

5.1.1 Heat transfer modes: Using a simplified model ignores more complex heat transfer interaction, for example, Durand de Gevigney *et al.* [6] introduced an additional heat transfer method, heat removal by centrifugal fling-off. Moreover, Changenet *et al.* [12] added an additional thermal resistance to their model; striction, which is where a constriction of the thermal current from the surface to the gear centre occurs.

The temperature probes in the gearbox could provide a source of error. They add an additional thermal mass and heat propagation channel which was not included in the thermal model.

5.1.2 Lubrication: The splash lubrication system relies on the rotation of the gears moving oil around the gearbox; the high-speed gears rely on the submerged low-speed shaft to distribute oil. From witnessing the gearbox during experimentation, it is effective in doing so. However, this means the chaotic nature of the lubrication system makes it difficult to model, especially the high-speed components as they are not in direct contact with the oil sump.

5.1.3 Data acquisition: The data acquisition system for this research used simple thermocouple sensors with an accuracy of ± 2°C in terms of uncertainty, as given in the specifications.

The design of the system had to account for the compact nature of the gearbox. Literature has found temperature measurement methods influence diagnostic capabilities, for example, data from thermography was found to be different from data from the contact sensor [5]. Therefore, subsequent research will consider a more sophisticated data acquisition system. With the aim of improving precision by repeating experiments and using sensors with increased sensitivity.

5.2 Future work

In addition to addressing the uncertainties previously discussed. Future work will involve validating gearbox faults experimentally by injecting known quantities of heat and inducing faults on test rig components. Also gathering data from a number of different operating conditions as changes to load will affect the thermal behaviour.

Using this thermal model in the context of condition monitoring will be an important further step. By posing the thermal model in a matrix format, it can then be inverted in a way so that temperature measurements can be used as an input to estimate losses at nodes. With a combination of temperature measurements, this could identify and locate a gearbox fault. Sensitivity analysis is required to determine how significant the uncertainties are in thermal modelling. Wemekamp and Luo [17] identified four input parameters for sensitivity analysis using a Monte Carlo method. They found radiation and air velocity impacted oil sump temperature most. This is something that can be explored in future work.

6 Conclusions

This paper demonstrates the potential for thermal modelling to be used as a wind turbine gearbox condition monitoring tool by understanding changes in thermal behaviour. A 'healthy' gearbox thermal model has been developed, modelling losses and heat transfer. The model was optimised and validated using experimental data and then used to mimic a component fault. It was found that single temperature measurements cannot necessarily detect or locate faults, but potentially a combination of temperature measurements could be used together to identify a gearbox fault. The method used in this paper allows further investigation into thermal behaviour of gearboxes as a result of a fault.

7 Acknowledgments

This work has been funded by the EPSRC, project reference number EP/L016680/1. The authors would like to acknowledge the work of Edward Hessell, Thorfinn Johnston, Paz Torres Noblejas, Steven Doherty and Ross Jamieson who collected the experimental data.

8 References

[1] Smolders, K., Feng, Y., Long, H., *et al.*: 'Reliability analysis and prediction of wind turbine gearboxes', presented at the European Wind Energy Conf., Warsaw, Poland, 2010

[2] Carroll, J., McDonald, A., Feuchtwang, J., *et al.*: 'Drivetrain availability in offshore wind turbines', in European Wind Energy Association 2014 Annual Conf., 2014

[3] de Azevedo, H.D.M., Araújo, A.M., Bouchonneau, N.: 'A review of wind turbine bearing condition monitoring: state of the art and challenges', *Renew. Sustain. Energy Rev.*, 2016, **56**, (Supplement C), pp. 368–379

[4] Qiu, Y., Feng, Y., Sun, J., *et al.*: 'Applying thermophysics for wind turbine drivetrain fault diagnosis using SCADA data', *IET Renew. Power Gener.*, 2016, **10**, (5), pp. 661–668

[5] Touret, T., Changenet, C., Ville, F., *et al.*: 'On the use of temperature for online condition monitoring of geared systems – a review', *Mech. Syst. Signal Process.*, Feb. 2018, **101**, (Supplement C), pp. 197–210

[6] Durand de Gevigney, J., Changenet, C., Ville, F., *et al.*: 'Thermal modelling of a back-to-back gearbox test machine: application to the FZG test rig', *Proc. Inst. Mech. Eng. Part J J. Eng. Tribol.*, Jun. 2012, **226**, (6), pp. 501–515

[7] British Standard: '*BS ISO/TR 14179-2:2001 gears - thermal capacity - Part 2: thermal load carrying capacity*' (British Standard, London, UK, 2001).

[8] Hoehn, B.-R., Michaelis, K., Hinterstoißer, M.: 'Optimization of gearbox efficiency', *GOMABN*, Jan. 2009, **488330184301821100**, pp. 441–480

[9] Velex, P., Ville, F.: 'An analytical approach to tooth friction losses in spur and helical gears— influence of profile modifications', *J. Mech. Des.*, Sep. 2009, **131**, (10), pp. 101008–101008–10

[10] Changenet, C., Oviedo-Marlot, X., Velex, P.: 'Power loss predictions in geared transmissions using thermal networks-applications to a Six-speed manual gearbox', *J. Mech. Des.*, 2006, **128**, pp. 618–625

[11] Fernandes, C.M.C.G., Marques, P.M.T., Martins, R.C., *et al.*: 'Gearbox power loss. Part II: friction losses in gears', *Tribol. Int.*, Aug. 2015, **88**, (Supplement C), pp. 309–316

[12] Changenet, C., Leprince, G., Ville, F., *et al.*: 'A note on flow regimes and churning loss modeling', *J. Mech. Des.*, Dec. 2011, **133**, (12), pp. 121009–121009–5

[13] Marques, P.M.T., Fernandes, C.M.C.G., Martins, R.C., *et al.*: 'Power losses at low speed in a gearbox lubricated with wind turbine gear oils with special focus on churning losses', *Tribol. Int.*, Jun. 2013, **62**, (Supplement C), pp. 186–197

[14] Fernandes, C.M.C.G., Marques, P.M.T., Martins, R.C., *et al.*: 'Gearbox power loss. Part I: losses in rolling bearings', *Tribol. Int.*, Aug. 2015, **88**, (Supplement C), pp. 298–308

[15] Zhao, H. s, Zhang, X. t: 'Early fault prediction of wind turbine gearbox based on temperature measurement'. 2012 IEEE Int. Conf. on Power System Technology (POWERCON), 2012, pp. 1–5

[16] Sheng, S., McDade, M., Errichello, R.: '*Wind turbine gearbox failure modes: a brief*', (National Renewable Energy Laboratory, Golden, CO, USA, 2011)

[17] Wemekamp, A.W., Luo, Y.: 'Efficiency and thermal gearbox calculation', in Int. Gear Conf. 2014: 26th–28th August 2014, Lyon, P. Velex, Ed. Chandos Publishing, Oxford, 2014, pp. 1069–1077